Control of the photoionization/photodissociation processes of cyclopentanone with trains of femtosecond laser pulses*

Song Yao-Dong(宋耀东), Chen Zhou(陈 洲), Yang Xue(杨 雪),
Sun Chang-Kai(孙长凯), Zhang Cong-Cong(张丛丛), and Hu Zhan(胡 湛)†

Institute of Atomic and Molecular Physics, Jilin University, Changchun 130021, *China*

(Received 3 February 2013; revised manuscript received 3 April 2013)

A train of three equally spaced femtosecond laser pulses is employed to control the photoionization/photodissociation processes of cyclopentanone. With the increase of pulse separation, a strong modulation of product ion yield is observed. More than ten-fold changes of ion yield ratio between different products can be realized. The experimental observations further explain the compositions and formation pathways of peaks in the mass spectra. The controlling mechanisms are also discussed.

Keywords: shaped femtosecond pulse, coherent control, time-of-flight mass spectra, photoionization and photodissociation

PACS: 33.80.R **DOI:** 10.1088/1674-1056/22/10/103301

1. Introduction

When lasers were invented they were considered as an ideal tool for controlling chemical reactions, i.e., selective cleavage or formation of chemical bonds.[1,2] However, the rapid internal vibrational energy redistribution (IVR) makes it difficult to use this approach to excite the bond of interest directly. Two approaches have been proposed for overcoming this obstacle. In the frequency domain, phase coherent control is proposed by Brumer and Shapiro,[3] in which a molecular state is excited by two different colored lasers and the yield is modulated by the relative phase of two pathways. In the time domain, femtosecond laser pulses are used to study chemical reaction dynamics,[4] which is known as femtochemistry.[5–7] The femtosecond laser pulse is not only an analytic tool,[8,9] but also an efficient way to control the molecular dynamics,[10,11] by optimizing the shape or phase of a pulse, which was proposed by Tannor and Rice.[12] Femtosecond pulse shaping is realized using spatial light modulators,[13] which are now popular experimental tools.[14,15]

There are two strategies for controlling molecular reaction dynamics using shaped femtosecond pulses: closed-loop and open-loop control. Due to the complexity of molecular systems, it is not generally possible to predict optimal control fields that will control the specified bond breaking and maximize the desired yield for a particular target. The closed loop strategy uses learning algorithms to find the solution to the molecule by an experimental system automatically. The method has been employed to control the relative fragmentation yields of molecules by many groups.[16,17] The method has been successfully used to control various processes, for example, ionization,[18] two-photon fluorescence,[19] and alignment.[20] While learning algorithms have been successful in discovering optimal laser pulses for control, it is generally difficult to understand the underlying physical mechanisms. Another strategy is to use the open-loop approach. Different shaped laser pulses can be obtained through using a variety of phase functions, e.g., a sequence of binary phases,[21] a variable π step function[22] or a sine phase function.[23] Using binary phase functions, isomers can be identified.[24] Dramatically different efficiencies of the SHG process can be achieved using the π step function.[25]

In this paper, a pulse train, which is obtained using a sine phase function, is employed to control photoionization and dissociation processes of cyclopentanone. The product yields and product yield ratios are controlled when the pulse separation in the train varies. The formation pathways of different products and the controlling mechanisms are discussed.

2. Experimental setup

The experimental setup, depicted schematically in Fig. 1, is similar to the one employed in our previous work.[26–28] Briefly, the laser system is a Ti:sapphire chirped-pulse amplification laser with a central wavelength at 800 nm, pulse duration of 90 fs, and repetition rate of 1000 Hz (Spitfire, Spectra-Physics). The laser beam is focused by a lens with a focal length of 225 mm into the vacuum chamber to interact with the C_5H_8O molecules. Commercial cyclopentanone (Aldrich Co. Ltd., 99% purity) is directly used without further purification. The sample with a pressure of 400 Pa is ejected through a pulsed nozzle into a vacuum chamber (background pressure of

*Project supported by the National Basic Research Program of China (973 Program) (Grant No. 2013CB922200), the National Natural Science Foundation of China, (Grant Nos. 10774056 and 10974070), the Fundamental Research Funds for the Central Universities, China (Grant No. 200903371), and the Specialized Research Fund for the Doctoral Program of Higher Education, China (Grant No. 20100061110045).

†Corresponding author. E-mail: huzhan@jlu.edu.cn

© 2013 Chinese Physical Society and IOP Publishing Ltd

2×10^{-5} Pa). The produced ions in the femtosecond laser field are collected by extraction and acceleration fields and detected by the dual micro-channel plate (MCP) detector at the end of the flight tube, and the signal is amplified by a preamplifier (ORTEC vt120) and sent to an oscilloscope (Tektronix, TDS 3054B). Each spectrum is an average of 64 laser shots. Then the data are sent to a computer.

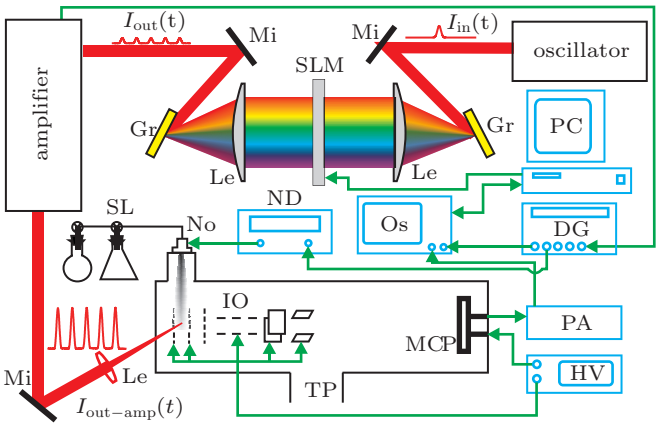


Fig. 1. (color online) Schematic diagram of the experimental setup. Transform-limited laser pulses from the laser oscillator are shaped using a spatial light modulator (SLM) before entering a laser amplifier. Components of the pulse shaping setup include lens (Le), grating (Gr), mirror (Mi), and SLM. The vacuum chamber, gas handling, and ion detection system components include a nozzle (No), a turbo pump (TP), a sample line (SL), ion optics (IO), and a microchannel plate (MCP). Electronic components include a nozzle driver (ND), an oscilloscope (Os), a delay generator (DG), a computer (PC), a preamplifier (PA), and a high voltage supply (HV).

The pulse shaping technique in the present work is similar to that used in our previous work, in which open-loop optimization[29] and closed-loop optimization[30] have been used to control the photoluminescence of gallium arsenide. The pulses are shaped by a 640-pixel dual-mask spatial light modulator (CRI Inc., SLM-640), using a standard configuration with four times the focal length. Two pairs of cylindrical lens (f = 300 mm) and grating (2000 grooves/mm) are used for spectrally dispersing (at the input) and recollimating (at the output) the laser pulses. A sine phase function is applied to the SLM to produce a pulse train, which is described in detail elsewhere.[29] A train of three equally spaced femtosecond laser pulses is used to control cyclopentanone molecular ionization and dissociation in our experiment. The MIIPS method[31] is used to ensure that a pulse without any phase is transform limited (TL).

3. Results and discussion

3.1. Controlling the ionization and dissociation products under the irradiation of pulse trains

A sequence of evenly spaced pulses is generated by using the sine phase function

$$\psi(\omega) = A\sin\left[(\omega-\omega_{\text{ref}})T+\phi\right], \qquad (1)$$

where amplitude A determines the number of pulses in the train, T determines the spacing between them, and ϕ is a constant phase offset.[29] A is chosen to be 1.2566 to generate a three pulse train, ϕ is fixed at 0, and T is scanned from 10.25 to 151.226 in this experiment, which corresponds to a pulse separation from 1.78 ps to 120 fs.

Figure 2(a) shows the mass spectrum of cyclopentanone under the irradiation of a transform-limited laser pulse at an intensity of 2×10^{13} W/cm^2. There is a series of peaks appearing at m/z (mass/charge) values of 1, 12∼15, 26∼29, 39∼43, 55, 72, 84 (the parent ion). When the molecule is irradiated by the pulse train, the shape of the spectrum changes as shown in Figs. 2(b)–2(f), with different pulse separations.

The values of the integrated peak intensity, I, of each peak are calculated. Figure 3 shows the peak intensities each as a function of pulse separation. For smaller products, with m/z equaling 1∼ 28, the overall intensities show a decreasing trend with pulse separation increasing. The values of the overall intensity of some other peaks do not change much, e.g., m/z equaling 29, 42. The intensity of peak 43 shows an increasing trend with pulse separation increasing. The overall intensities of larger products, e.g., m/z equaling 55, 72, and 84, increase first, reach their maxima near 0.8 ps∼1 ps, then decrease at even longer pulse separation. Besides the overall intensity trend, we observe the strong modulations for some of the peaks, e.g., m/z equaling 1, 15, 27, etc. Some of the modulation curves (for example, m/z equaling 15 or 27 as shown in Fig. 3) can be fitted well with a sine wave with decreasing amplitude and average intensity as the following equation:

$$f(x) = A_1\,\mathrm{e}^{-x/x_{01}}\sin(2\pi x/T+\phi)+y_0+A_2\,\mathrm{e}^{-x/x_{02}}, \qquad (2)$$

A T (sine wave period) value of 280 fs is obtained from the fitting. The modulations of some other peaks are obscure, e.g., m/z equaling 39, etc. If we compare different curves in Fig. 3, we can see that the peaks and dips of modulated curves do not always fall at the same place. For example, at a pulse separation of 0.198 ps, curves with m/z equaling 1, 15, and 27 etc. are in the dips, curves with m/z equaling 39, 84 etc. are at the peaks. An overall trend is that the curves with large m/z values tend to have opposite peak and dip positions to the curves with small m/z values. However, for some medium m/z value peaks, the trend is not very clear. For example, we just show that at 0.198 ps the curve with m/z equaling 39 is at the peak, the same as the curve of the parent ion. But at 0.446 ps, the curve with m/z equaling 39 is in the dip, which is the same as some peaks with smaller m/z values, opposite to the curve of the parent ion. Thus, we choose a few typical pulse separation values in the dips and at the peaks to compare the mass spectrum shapes at these positions. These mass spectra are shown in Figs. 2(b)–2(e), for pulse separations of 0.198 ps, 0.279 ps, 0.446 ps, and 0.585 ps. A mass spectrum at a longest pulse separation value, 1.779 ps, is also shown in Fig. 2(f).

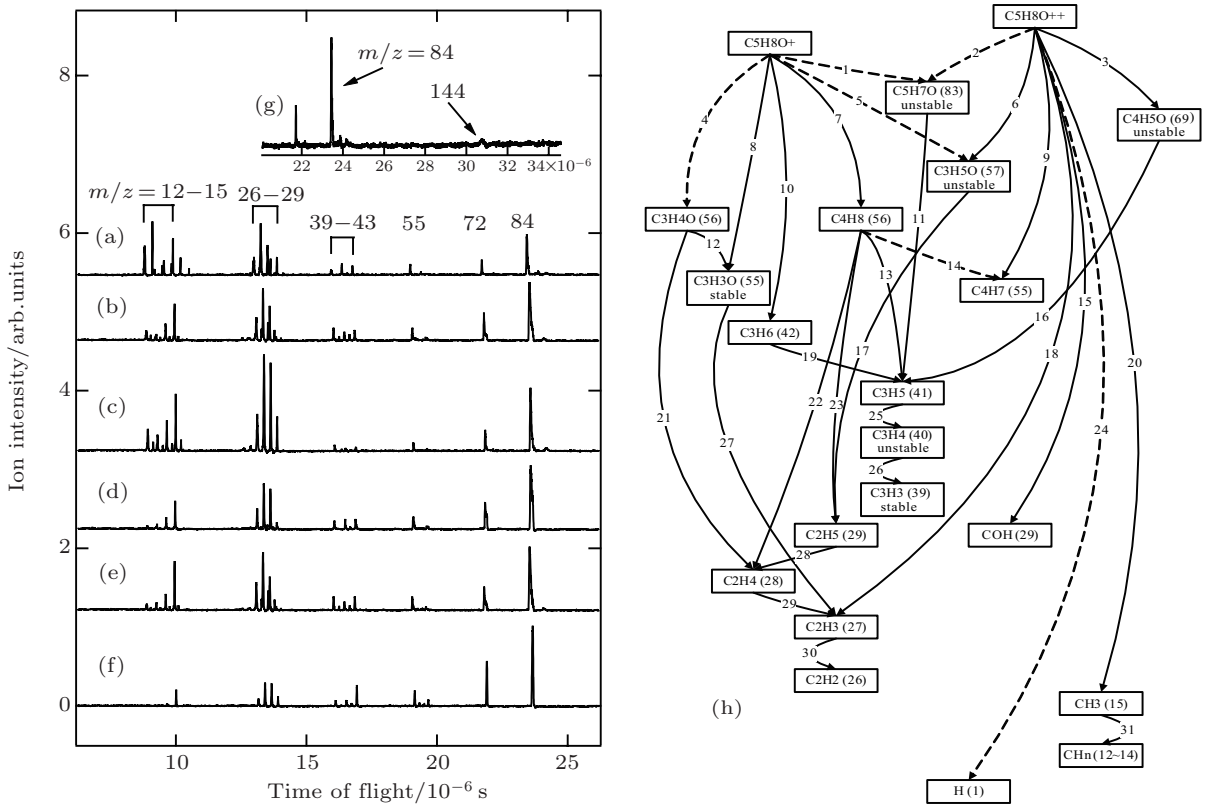


Fig. 2. Time of flight mass spectra of cyclopentanone under the irradiation of (a) transform-limited pulse, and pulse trains with pulse separation values of (b) 0.198 ps, (c) 0.279 ps, (d) 0.446 ps, (e) 0.585 ps, (f) 1.779 ps. $m/z = 1$ peak is not shown here for the clarity of the rest of the peaks. Inset (g) shows a peak appearing at 30.8 μs with $m/z = 144$. Panel (h) shows the reaction pathways of cyclopentanone in a femtosecond laser field summarized from Ref. [27]. Products are shown in boxes with their m/z values in parentheses. Curves with arrows link reactants with their products. Dashed line pathways are for relatively low branching ratios.

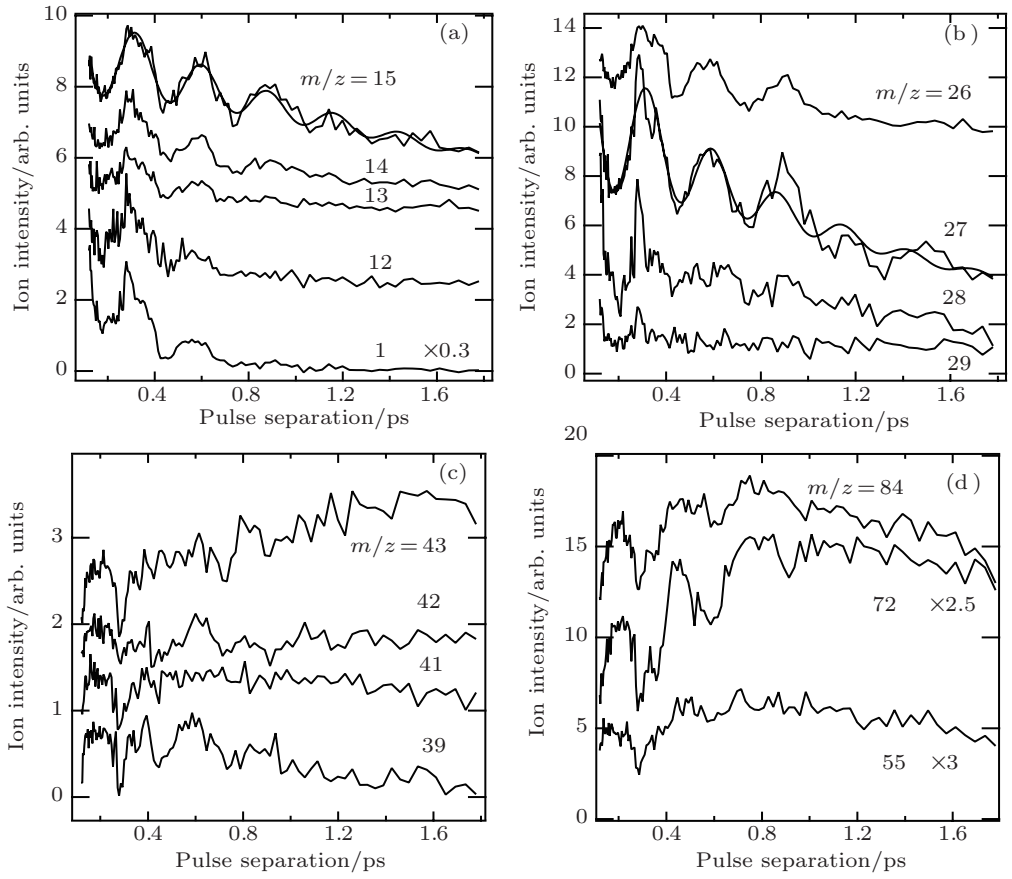


Fig. 3. Intensities of mass peaks in the spectra, each as a function of pulse separation. Curves are shifted vertically for the purpose of clarity. The smooth curves overlapped with curves of m/z equaling 15 and 27 are fits to Eq. (2).

For a modulated curve, like one of those shown in Fig. 3, we define modulation depth M as

$$M = (I_{\max} - I_{\min})/(I_{\max} + I_{\min}), \tag{3}$$

in which $I_{\max}$ and $I_{\min}$ are maximal and minimal intensities on the modulation curve, respectively. Larger modulation depth means more effective control. A modulation depth of 100% means that the product channel can be switched on or off by adjusting experimental variables. We take the maximum or minimum intensity around the pulse separation of 0.198 ps or 0.279 ps as $I_{\max}$ or $I_{\min}$, and calculate the modulation depths for each mass peak around this position, and their results are listed in Table 1. We see a maximal modulation depth of 78.9% for m/z equaling 12 and a minimal modulation depth of 14.51% for m/z equaling 84. Thus, by adjusting the period of sine phase function applied to the femtosecond laser spectrum, we achieve the effective control of the ionization and dissociation products of cyclopentanone.

Table 1. Modulation depths for each peak in mass spectra. $I_{\max}$ and $I_{\min}$ are in arbitrary units.

Mass peak (m/z)	$I_{\max}$	$I_{\min}$	M
1	10.276	3.5119	49.06%
12	3.5093	0.4139	78.90%
13	1.7995	0.49336	56.97%
14	2.9266	1.3314	37.46%
15	4.7227	2.6676	27.81%
26	5.0881	2.5355	33.48%
27	11.917	6.2462	31.22%
28	9.3741	3.812	42.18%
29	2.705	0.88125	50.85%
39	1.4197	0.61703	39.41%
41	1.0633	0.28086	58.21%
42	0.7239	0.14055	67.48%
43	1.3603	0.35375	58.72%
55	1.7487	0.81391	36.48%
72	4.4705	2.3777	30.56%
84	16.94	12.647	14.51%

The ion yield ratio between different products can be changed dramatically by changing the phase applied to laser spectrum. For example, we now look at the ion intensities of m/z equaling 12, 55, and 84 at the pulse separations of 0.198 ps and 0.279 ps. I_{nn} denotes the intensity of mass peak with m/z equaling nn. At 0.198 ps, $I_{84}/I_{12} = 40.92$. At 0.279 ps, this ratio becomes 3.60. Thus, by changing applied phase, or changing the pulse separation, the product yield ratio changes by 11.37 fold. Similarly, at 0.198 ps, $I_{55}/I_{12} = 4.225$, the ratio becomes 0.232 at 0.279 ps. The product yield ratio changes by 18.23 fold.

The intensity of each peak when the molecule is irradiated with pulse train is also compared with that when irradiated with transform-limited pulse. If only laser pulse width is considered, the yield of a multiphoton process would decrease with pulse width increasing. In our experiments, the effective pulse width[32] of the pulse trains is larger than that of a TL pulse, even at the smallest pulse separation. However, we observed intensity enhancement for most of the products except those with m/z equaling 1, 12, and 13. The ratio matrix of each peak intensity at a certain pulse separation to that peak intensity under the irradiation of TL pulse is plotted in Fig. 4. The largest enhancement, at a ratio of 7.47, is observed for the case with mass peak m/z equaling 42, which is a very small peak under the irradiation of TL pulse. Its intensities are increased dramatically when the pulse separation are set at 0.198 ps and 0.585 ps as can be seen from Figs. 2(b) and 2(e). For other prominent mass peaks, we also observed strong enhancement, e.g., ratio of 2.67 for m/z equaling 84, 4.92 for m/z equaling 72, 2.21 for m/z equaling 28, etc.

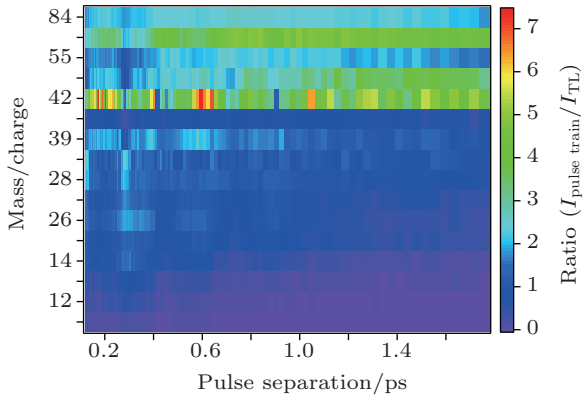


Fig. 4. (color online) The ratios of mass peak intensity under the irradiation of pulse train ($I_{\text{pulse train}}$) to that under the irradiation of TL pulse (I_{TL}), each as a function of pulse separation, for each peak in the mass spectra.

3.2. Reaction pathways of cyclopentanone

The reaction dynamics of cyclopentanone in a femtosecond laser field has been studied by a few groups.[33–35] In our previous work,[27] we have used the Rice–Ramsperger–Kassel–Marcus (RRKM)[36] theory with the potential surfaces obtained from the *ab initio* quantum chemical calculations to interpret how the products are formed. Here, new data from pulse train experiments enable us to explain the reaction pathways more precisely. All possible reaction pathways summarized from our previous work[27] are illustrated in Fig. 2(h). Next, we analyze each mass peak, assign it to a particular fragment, and discuss its formation pathways.

The peak at m/z equaling 55 can correspond to $C_3H_3O^+$ or $C_4H_7^+$. There are four pathways forming m/z equaling 55 products in Fig. 2(h), i.e., processes 8, 12, 9, and 14. The possibility of forming from pathway 12 is small because pathway 4 is weak and the amount of product $C_3H_4O^+$ is small. Pathway 14 is weak. So the m/z equaling 55 peak can either be $C_3H_3O^+$ forming from the parent ion through pathway 8 or $C_4H_7^+$ forming from parent dication through pathway 9. In Fig. 3, we can see that at a smaller pulse separation, the dip

and peak positions of the curve with m/z equaling 55 are the same as those of parent ion. Hence, at small pulse separation, the m/z equaling 55 peak originates mostly from $C_3H_3O^+$ dissociated from the parent ion. With the increase of pulse separation, the shape of the curve with m/z equaling 55 gradually differs from that of the parent ions, and becomes chaotic. We notice that the signal intensity does not decrease, instead it increases compared with that at smaller pulse separation. So this chaotic shape of the curve is not caused by low signal-to-noise ratio. It is an indication of increasing contribution from another product $C_4H_7^+$ dissociated from parent dication. The modulation is washed out because the maximum and minimum positions of parent ion are opposite to those of parent dication intensities. We will see more evidences of this while analyzing the origin of other mass peaks, and we will discuss possible mechanisms of it in the following section.

There are a few peaks appearing at m/z equaling 39∼42. As seen in Fig. 2(h), the only pathway forming product with m/z equaling 42 is the dissociation of a parent ion into $C_3H_6^+$ (pathway 10). Another possibility for the origin of this peak is the parent dication. These two pathways, one coming from the parent ion and the other from parent dication, make the modulation curve rather chaotic. There are four possible origins for the peak ($C_3H_5^+$) with m/z equaling 41. The first one is H loss from $C_3H_6^+$ through pathway 19. The second one is the dissociation from $C_4H_8^+$ through pathway 13. The third one is the dissociation from unstable $C_4H_5O^+$ through pathway 16. The fourth one is the dissociation from unstable $C_5H_7O^+$ through pathway 11. The fourth pathway is weak since the amount of $C_5H_7O^+$ from pathways 1 and 2 is very small. The first two pathways are the secondary dissociation of parent ion products. The third pathway is the secondary dissociation of the parent dication product. Again, the contributions from both parent ion and parent dication result in a chaotic modulation curve in shape. There is only one pathway to form $C_3H_4^+$, that is, H loss from $C_3H_5^+$. The $C_3H_4^+$ is unstable, resulting in a very weak mass peak. It will lose H to form $C_3H_3^+$ easily. The $C_3H_3^+$ is a stable product.

Another series of peaks appears at m/z equaling 26–29. One possible product corresponding to m/z equaling 29 is $C_2H_5^+$, it can be formed from the dissociation of $C_4H_8^+$ through pathway 23, or from the dissociation of $C_3H_5O^+$ through pathway 17, they are secondary dissociations of parent ion and parent dication, respectively. Another possible product of 29 is COH^+, it is the direct dissociation product from parent dication. The mass peak corresponding to m/z equaling 28 is $C_2H_4^+$. It can be formed by H loss from $C_2H_5^+$ through pathway 28, or dissociation of $C_4H_8^+$ through pathway 22. Pathway 21 is weak since the amount of $C_3H_4O^+$ formed through pathway 4 is small. The $C_2H_3^+$ (m/z = 27) can be formed by direct dissociation of parent dication through pathway 18. Another possibility is from the dissociation of $C_3H_3O^+$. However, $C_3H_3O^+$ is a pretty stable product, so the contribution from this pathway is small. It is shown in Ref. [37] that the H loss reaction from $C_2H_4^+$ to form $C_2H_3^+$ needs to overcome a high barrier of 107 kcal/mol. Hence the contribution from pathway 29 is also small. $C_2H_2^+$ ($m/z = 26$) can only be formed by H loss from $C_2H_3^+$. From the above discussion, we see that the products with m/z equaling 28 and 29 both have contributions from parent ion and parent dication, so we can see rather chaotic shapes of their modulation curves in Fig. 3. The peak with m/z equaling 27 ($C_2H_3^+$) can only be formed directly from parent dication. Though it is only 1 m/z value difference, it is not the product of $C_2H_4^+$. Thus, the shapes of the curves with m/z equaling 26 and 27 differ dramatically from those with m/z equaling 28 and 29, the modulations are very clear. The dips and peaks of the modulations are opposite to those of the parent ion, because they are contributed to only by parent dication.

The CH_3^+ ($m/z = 15$) is the direct dissociation product of parent dication. And CH_n^+ ($n = 0 \sim 2$) are the products by successive H loss. So the modulation curves of these products follow the same oscillation phase as those produced from parent dication. The H^+ ion can be formed from the parent dication dissociation, but it is a minor product. Or it can be formed by the dissociation of dications produced by ionizing primary products. These primary products must be mainly from parent dication since the oscillation phase of H^+ follows those products from parent dication.

We will now discuss some other peaks observed in the mass spectra. In most of other work, the peak at m/z equaling 72 was not observed. In Wu *et al.*'s work,[33] the peak was observed, but the origin was not discussed. In our calculations in previous work,[27] we did not find any pathway forming this product from unimolecular reaction, either. In the mass spectra, at longer flight time, we can see a very small peak at m/z equaling 144 as shown in Fig. 2(g). If it originates from cyclopentanone, this product can be formed only from a cluster since its m/z is larger than that of the parent ion. Thus, we speculate that the formation of the product with m/z equaling 72 is a cluster mediated process, i.e., the molecules form a dimer, and the dimer loses two carbon atoms after which it dissociates into $C_4H_8O^+$ ($m/z = 72$). Another possibility that could form the product with m/z equaling 72 is that the product with m/z equaling 144 is an impurity in the vacuum chamber and that with m/z equaling 72 is its doubly charged ion. However, under the relatively low laser intensity in current experiment condition (2×10^{13} W/cm^2), we expect to see the

laser intensity for the case of doubly charged ion to be smaller than for the case of singly charged ion. On the contrary, in the mass spectra, the peak with m/z equaling 72 is always much larger than the one with m/z equaling 144. Furthermore, the peak with m/z equaling 72 is too strong to be regarded as a peak originating from an impurity. Further experimental and theoretical studies are needed to determine the true origin of this product, for example, an experiment with higher sample concentration to form more clusters, and theoretical calculations of the cluster structures.

The mass peak at m/z equaling 43 could be due to the impurity of acetone in the chamber. The acetyl ion (CH_3CO^+) is a typical product from acetone. However, in our experiments of acetone, under the present experimental conditions, the peak intensity of an acetyl ion is much smaller than that of the parent ion at m/z equaling 58, which is contrary to what we see in the present mass spectra. So this peak with m/z equaling 43 should not be a product from impurity. We speculate that it is a dissociation product from $C_4H_8O^+$ discussed above. If we look at the modulated curves in Fig. 3, the curve with an m/z value of 43 is not similar to those with m/z values of 39, 41, and 42, but it is rather similar to that with an m/z value of 72. Firstly, they both increase in intensity with pulse separation increasing. Secondly, their oscillations look similar, especially the one around 0.8 ps, which is absent in the curves of 39, 41, and 42.

3.3. Possible controlling mechanisms

We propose two possible controlling mechanisms to explain the modulation of the ion intensity observed while increasing pulse separation.

The first mechanism is the multiphoton intrapulse interference (MII).[38] In a multiphoton process, an excited molecular state can be reached by different combinations of different frequency photons within the band width of femtosecond laser, as long as the sum of energies of those photons equals the energy difference between upper and lower states. If photons of different frequencies have different phases, the phases can add up constructively or destructively, the multiphoton process at a certain wavelength or as a whole in the band width can be enhanced or suppressed. In an n-th order multiphoton process, the electric field spectrum can be calculated by the following equation:[39]

$$\begin{aligned} A^{(n)}(\Delta) \propto & \int_{-\infty}^{+\infty} \cdots \int_{-\infty}^{+\infty} \mathrm{d}\Omega_1 \cdots \mathrm{d}\Omega_{n-1} \, |E(\Omega_1)| \cdots |E(\Omega_{n-1})| \\ & \times |E(\Delta - \Omega_1 \cdots - \Omega_{n-1})| \\ & \times \exp\left[\mathrm{i}\left\{\varphi(\Omega_1) \cdots + \varphi(\Omega_{n-1}) \right.\right. \\ & \left.\left. + \varphi(\Delta - \Omega_1 - \Omega_{n-1})\right\}\right], \end{aligned} \tag{4}$$

where Ω_i is the fundamental frequency in the laser spectrum, Δ is the frequency in the n-th order spectrum, $|E(\Omega_i)|$ and $\varphi(\Omega_i)$ are the spectrum amplitude and phase at Ω_i, respectively. Using our laser spectrum and the applied phase, the two- and three-photon electric field spectra are calculated at each pulse separation value (i.e., the T value in Eq. (1) for the sine function phase applied). Figure 5 shows the spectrum amplitude at 402.3 nm for the two-photon spectrum and integrated spectrum amplitude for the whole three-photon spectrum, each as a function of pulse separation. We see that the multiphoton electric field spectrum is strongly modulated and the processes of different numbers of photons possess different characteristics of the modulations, i.e., the modulation period, the modulation phase, the modulation depth and its decay. Thus, we speculate that at the multiphoton levels that form the parent ion and the present parent dication, MII caused modulations of the spectrum in the way that parent ion and parent dication are enhanced or suppressed are opposite to each other. The energy levels of a molecule with size like cyclopentanone are very complex, the molecule requires many more photons to reach the parent ion and parent dication levels, and the calculation of the yield of a multiphoton process using its electric spectrum and absorption spectrum will require a lot of work to be done.

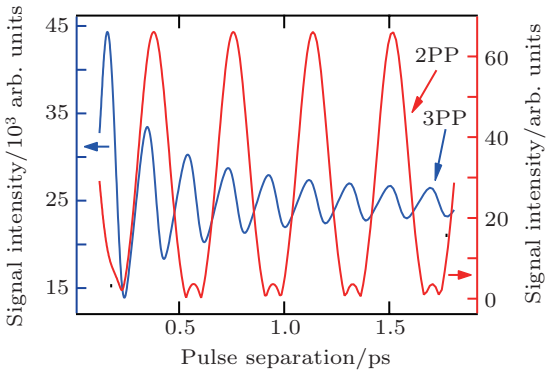


Fig. 5. (color online) Intensities of 402.3 nm in the calculated two-photon process (2PP) electric field spectrum and integrated intensity of three-photon process (3PP) spectrum, each as a function of pulse separation.

The above mechanism is used to treat the problem in the frequency domain by considering the interference of different frequency photons. The next mechanism will be used to treat the problem in the time domain, in which a wave packet is created by the first pulse in the train and is matched by following pulses in the train to form products. The time when the following pulses arrive determines the yield of the products. In our preliminary study, the absorption spectrum of parent dication with an open ring $CH_3CHCH_2CH_2CO^{++}$ structure is calculated, using the B3LYP method, at a 6-31++G (d, p) level. The calculations are carried out by using a Gaussian 03 program.[40] The CH–CH_2 bond length in the stable

structure of $CH_3CHCH_2CH_2CO^{++}$ is 1.47581 Å. We increase this bond length in steps of 0.05 Å, and optimize the structure at each step. As shown in Fig. 6, the absorption (oscillator strength) of parent dication around 200 nm decreases from 0.2311 at 1.47581 Å, to 0.0267 at 1.87191 Å. Thus, while the wave packet is oscillating on the potential energy surface, we expect to see an oscillation of its product yields with pulse separation increasing, because of the absorption change.

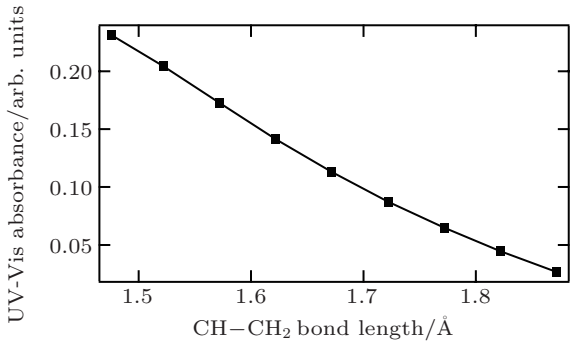


Fig. 6. Absorption of parent dication around 200 nm as a function of CH–CH_2 bond length.

4. Conclusions

We have investigated the photoionization and photodissociation of cyclopentanone using shaped femtosecond laser pulses. Under the irradiation of the pulse trains of three equally spaced pulses, with the increase of pulse separation, strong modulation with a modulation depth as large as 78.9% of the product ion yield is observed. The peaks and dips of modulation curves of different products sometimes fall at places opposite to each other. Hence, a change of product ion yield ratio between different products can be realized by changing pulse train parameters. Changes of the ratio are observed to reach as large as 11 and 18 folds for I_{84}/I_{12} and I_{55}/I_{12}, respectively. Based on the experimental observations from controlling experiments, the compositions and formation pathways for different peaks in mass spectra are assigned. Finally, we proposed two possible mechanisms for the controlling of photoionization and photodissociation processes observed in the present study, which are based on the multiphoton intrapulse interference and the oscillation of a wavepacket on the potential energy surface.

References

[1] Damrauer N H, Dietl C, Krampert G, Lee S H, Jung K H and Gerber G 2002 *Eur. Phys. J. D* **20** 71
[2] Gordon R J and Rice S A 1997 *Ann. Rev. Phys. Chem.* **48** 601
[3] Brumer P and Shapiro M 1986 *Chem. Phys. Lett.* **126** 541
[4] Carley R E, Heesel E and Fielding H H 2005 *Chem. Soc. Rev.* **34** 949
[5] Zewail A H 2000 *Angew. Chem. Int. Ed.* **39** 2586
[6] Zewail A H 1993 *J. Phys. Chem.* **97** 12427
[7] Zewail A H 2000 *Pure Appl. Chem.* **72** 2219
[8] Chen D Y, Zhang S and Xia Y Q 2009 *Chin. Phys. B* **18** 3073
[9] Guo W, Zhu J Y, Wang B X, WangY Q and Wang L 2009 *Chin. Phys. Lett.* **26** 013201
[10] Zhang S A, Wang Z G and Sun Z R 2008 *Chin. Phys. B* **17** 2914
[11] Qin C C, Zhao X D, Zhang X Z and Liu Y F 2013 *Chin. Phys. Lett.* **30** 023302
[12] Tannor D J and Rice S A 1985 *J. Chem. Phys.* **83** 5013
[13] Weiner A M 2000 *Rev. Sci. Instrum.* **71** 1929
[14] Xu Y, Zhang S A, Zhang L, Sun Z R, Zhang X Y, Chen G L, Wang Z G, Li R X and Xu Z Z 2005 *Chin. Phys. Lett.* **22** 2557
[15] Plenge J, Wirsing A, Drebenstedt I W, Halfpap I, Kieling B, Wassermann B and Ruhl E 2011 *Phys. Chem. Chem. Phys.* **13** 8705
[16] Assion A, Baumert T, Bergt M, Brixner T, Kiefer B, Seyfried V, Strehle M and Gerber G 1998 *Science* **282** 919
[17] Levis R J, Menkir G M and Rabitz H 2001 *Science* **292** 709
[18] Cardoza D, Baertschy M and Weinacht T 2005 *J. Chem. Phys.* **123** 074315
[19] Zhang S A, Sun Z R, Zhang X Y, Xu Y, Wang Z G, Xu Z Z and Li R X 2005 *Chem. Phys. Lett.* **415** 346
[20] Nalda R D, Horn C, Wollenhaupt M, Krug M, Banares L and Baumert T 2007 *J. Raman Spectrosc.* **38** 543
[21] Pastirk I, Kangas M and Dantus M 2005 *J. Phys. Chem. A* **109** 2413
[22] Oron D, Dudovich N and Silberberg Y 2003 *Phys. Rev. Lett.* **90** 213902
[23] Wollenhaupt M, Präkelt A, Tudoran C S, Liese D, Bayer T and Baumert T 2006 *Phys. Rev. A* **73** 063409
[24] Cruz J M D, Lozovoy V V and Dantus M 2005 *J. Phys. Chem. A* **109** 8447
[25] Wnuk P and Radzewicz C 2007 *Opt. Commun.* **272** 496
[26] Wu D, Wang Q Q, Cheng X H, Jin M X, Li X Y, Hu Z and Ding D J 2007 *J. Phys. Chem. A* **111** 9494
[27] Wang Q Q, Wu D, Jin M X, Liu F C, Hu F F, Cheng X H, Liu H, Hu Z, Ding D J, Mineo H, Dyakov Y A, Mebel A M, Chao S D and Lin S H 2008 *J. Chem. Phys.* **129** 204302
[28] Song Y D, Chen Z, Sun C K and Hu Z 2013 *Chin. Phys. B* **22** 013302
[29] Hu Z, Singha S and Gordon R J 2010 *Phys. Rev. B* **82** 115204
[30] Singha S, Hu Z and Gordon R J 2011 *J. Phys. Chem. A* **115** 6093
[31] Hou B, Easter J H, Nees J A, He Z, Thomas A G R and Krushelnick K 2012 *Opt. Lett.* **37** 1385
[32] Suzuki T, Sugawara Y, Minemoto S and Sakai H 2008 *Phys. Rev. Lett.* **100** 033603
[33] Wu C Y, Xiong Y J, Wang J X and Kong F A 2000 *Chin. Chem. Lett.* **11** 545
[34] Kosmidis C, Tzallas P, Ledingham K W D, Mccanny T, Singhal R P, Taday P F and Langley A J 1999 *J. Phys. Chem. A* **103** 6950
[35] Kosmidis C, Philis J G and Tzallas P 1999 *Phys. Chem. Chem. Phys.* **1** 2945
[36] Klippenstein S J 1992 *J. Chem. Phys.* **96** 367
[37] Satyapal S, Johnston G W, Bersohn R and Oref I 1990 *J. Chem. Phys.* **93** 6398
[38] Lozovoy V V, Pastirk I and Dantus M 2004 *Opt. Lett.* **29** 775
[39] Walowicz K A, Pastirk I, Lozovoy V V and Dantus M 2002 *J. Phys. Chem. A* **106** 9369
[40] Frisch M J, Trucks G W, Schlegel H B, Scuseria G E, Robb M A, Cheeseman J R, Montgomery J A, Vreven T Jr, Kudin K N, Burant J C, Millam J M, Iyengar S S, Tomasi J, Barone V, Mennucci B, Cossi M, Scalmani G, Rega N, Petersson G A, Nakatsuji H, Hada M, Ehara M, Toyota K, Fukuda R, Hasegawa J, Ishida M, Nakajima T, Honda Y, Kitao O, Nakai H, Klene M, Li X, Knox J E, Hratchian H P, Cross J B, Adamo C, Jaramillo J, Gomperts R, Stratmann R E, Yazyev O, Austin A J, Cammi R, Pomelli C, Ochterski J W, Ayala P Y, Morokuma K, Voth G A, Salvador P, Dannenberg J J, Zakrzewski V G, Dapprich S, Daniels A D, Strain M C, Farkas O, Malick D K, Rabuck A D, Raghavachari K, Foresman J B, Ortiz J V, Cui Q, Baboul A G, Clifford S, Cioslowski J, Stefanov B B, Liu G, Liashenko A, Piskorz P, Komaromi I, Martin R L, Fox D J, Keith T, Al-Laham M A, Peng C Y, Nanayakkara A, Challacombe M, Gill P M W, Johnson B, Chen W, Wong W, Gonzalez C and Pople J A 2003 *Gaussian* 03 (Pittsburgh PA: Gaussian Inc.,)